Materials Physics and Mechanics. 2023;51(7): 107-116
Research article
http://dx.doi.org/10.18149/MPM.5172023_9

Submitted: April 12, 2023
Approved: July 12, 2023
Accepted: October 31, 2023

Assessment of physical and vibration damping characteristics of sisal/PLA biodegradable composite

Y. Munde [1], A.S. Shinde [1] ✉, I. Siva [2], P. Anearo [3]

[1] MKSSS's Cummins College of Engineering for Women, Maharashtra, India

[2] Rajas Institute of Technology, Tamilnadu, India

[3] Vishwakarma Institute of Information Technology, Maharashtra, India

✉ avinash.shinde@cumminscollege.in

Abstract. Natural fiber composites have industrially attractive because of their low density, low cost, and comparable specific mechanical properties with synthetic fiber. The extrusion and injection molding method is used to fabricate the sisal fiber-reinforced PLA biodegradable composites with random fiber orientations. The fiber weight fraction varied from 0 to 30 wt. % (in the step of 10 %), and the influence of the fiber weight fraction of biocomposite on different properties was studied. The composites are tested for evaluating the physical properties, viz. density, hardness, and water absorption and vibration characteristics, viz. natural frequency and damping ratio. The density of Sisal/PLA biocomposites was seen from 1.18 to 1.23 gm/cm^3 and hardness from 93.84 to 97.28. In water absorption, as the weight percentage of sisal increases, the diffusion and permeability coefficient increase and reach 2.83E-05 and 8.11E-06, respectively, for 30 % sisal loading. The fundamental natural frequencies and damping ratio of 30 wt. % sisal fiber biocomposite are 24.41 Hz and 0.1450, respectively, higher than the pure PLA. This is observed for all vibration modes, and the reason behind this is the high stiffness of fibers. These developed biodegradable composites help lower the cost of purePLA-based composites and have wise applications in packaging and allied industries.
Keywords: natural frequency; damping ratio; sisal fiber; PLA; water absorption

Citation: Munde Y, Shinde AS, Siva I, Anearo P. Assessment of physical and vibration damping characteristics of sisal/PLA biodegradable composite. *Materials Physics and Mechanics.* 2023;51(7): 107-116. DOI: 10.18149/MPM.5172023_9.

Introduction

A highly demanded and exponentially raised use of synthetic fiber reinforced composites in industries posed environmental concerns because of their non-degradable and non-renewable properties. Industries are looking to develop green materials independent of polymers derived from petroleum resources (1). Among the different biopolymers available today, i.e. polyhydroxy butyrate (PHB), poly(hy- droxyalkanoate) (PHA), polybutylene succinate (PBS), poly(lactic acid), starch, polycaprolactone (PCL), the PLA is promising to replace petroleum-based polymer in engineering applications which are renewable and biologically degradable because made from the fermentation of starch-based biomass. Initially, the high cost of PLA ed its use, but recently the cost has recentlys use, but recently the cost has fallen. The reinforcement of natural fibers in PLA producess composites with enhanced properties and also minimizes the amount of PLA required, which saves cost (2).

Publisher: Peter the Great St. Petersburg Polytechnic University

Several studies were carried out on the static mechanical behavior of PLA composites with a different types of natural fiber such as sisal [1,3,4], jute [5–8], Banana [4,9–13], pulp fibers (14), Pineapple Leaf (15), Ramie fabric [16,17], oil palm (18), corn (19), sugarcane bagasse (20), Grewia optiva (21), flax [22,23], kenaf (24), bamboo (25), Waste Leather Buff (26), olive pit powder (27). In comparison, many of these researchers have studied the effect of fiber loading, treatment of fiber, and fiber length on mechanical behavior in terms of tensile, flexural, and impact properties. They show that natural fibers reinforcement in PLA composites has good potential.

The literature reveals that a large quantum of research was carried out on sisal/PLA composite, but minimal work is reported on the vibration-damping behavior of biodegradable composites. The present work attempts to fabricate sisal/PLA composites using an extrusion-injection molding process with different weight fractions of sisal fiber. Experimental modal analysis will characterize the fabricated composite for physical and vibration properties.

Materials and Methods

PLA matrix and sisal fiber property details. The matrix used in this study is Ingeo biopolymer polylactic acid (PLA) of grade 3052D, supplied by Nature Works LLC, USA. This is designed for injection molding applications with a density of 1.24 g/cc, MFI 14 g/10 min (at 210 °C/2.16 Kg). Sisal fibers are obtained from the sisal plant leaves *Agave sisalana*. Fiber is extracted by a process known as decortication. The sisal fibers were obtained from Tokyo Engineering Corporation, Coimbatore, India. The chemical composition of sisal fiber includes 66-72 % cellulose, 12 % hemicellulose, 10-14 % lignin, and 11 % moisture content. The physical and mechanical properties of sisal fiber and PLA matrix are listed in Table 1.

Table 1. Properties of sisal fiber and PLA matrix

Property	**Sisal fiber**	**PLA matrix**
Density, g/cc	1.45	1.24
Elongation, %	2-2.5	3.5
Tensile strength, MPa	511-635	62
Young's modulus, GPa	9.4-22	-
Heat distortion temperature, °C	-	55

Manufacturing of specimens. Overnight dried sisal fibers of 3 to 5 mm, and PLA was compounded using a twin screw extruder (Make M/s Specific Engineering, Model –ZV 20) with Screw diameter 21 mm, L/D ratio 40:1, zonal temperature 165-210 °C and speed 40 rpm. Pallets were produced for 0, 10, 20, and 30 wt. % of fiber to the polymer weight. Table 2 shows the specimen coding followed in the production. Extruded pallets were dried at 90 °C for 12 hr. in a hot air-oven and then injection molded by injection molding machine (Make Ferromatik Milacron, model-OMEGA 80W) with a screw diameter of 36 mm and screw speed of 298 rpm. The molding temperature ranged from 175 to 200 °C, and a pressure of 50 bar was maintained.

Table 2. Composites formulation for specimen preparation

Composite designation	Weight fraction of sisal fiber, %	Weight fraction of PLA matrix, %
PLA	0	100
S10	10	90
S20	20	80
S30	30	70

Experimental studies

Measurement of density and void content. The density measurement of sisal/PLA composites as found out using Archimedes' principle. Theoretical density (ρ_t) of was calculated using Eq. (1):

$$\rho_C = \frac{1}{\left(\frac{W_f}{\rho_f} + \frac{W_m}{\rho_m}\right)}, \quad (1)$$

where ρ_c, ρ_f, and ρ_m are the densities of composites, fiber and matrix, respectively. The weight fraction of fiber and matrix denoted are by W_f and W_m.

The volume of void fraction (V_v) of the sisal/PLA composites was calculated from values of experimental and theoretical densities by Eq. (2):

$$V_v = \frac{\rho_t - \rho_e}{\rho_t}. \quad (2)$$

Measurement of shore D hardness. The Shore *D* hardness of PLA and sisal/PLA composites was measured using a digital Durometer HT-6510D. The hardness is measured as per ASTM D2240 at three different points, and the average value is reported.

Water absorption test. The specimens of sisal/PLA composites of dimensions 20 × 20 mm were used to measure water absorption as per ASTM D570. The specimens of all compositions were dried in a hot air oven at 80 °C for 12 hr. to remove moisture content. The completely dried specimen was immersed in distilled water for 7 days with an interval of 24 hr. Every 24 hr. of time, specimens were taken out from the water, wipedd out to remove excess water and immediately measured weight with an analytical weighing balance. Eq. (3) is used to calculate % of water absorption:

$$WA(\%) = \frac{W_t - W_1}{W_1}, \quad (3)$$

where W_t and W_1 are the weight of the specimen for a different time and the sample's initial dry weight, respectively.

The kinematics of water can be understood by calculating parameters such as the Diffusion coefficient (D) and Sorption coefficient (S) using Eqs. (4) and (5), respectively:

$$D = \frac{t^2 m^2}{16 W_\infty{}^2}, \quad (4)$$

$$S = \frac{W_\infty}{W_t}, \quad (5)$$

where t is the initial sample thickness, m is the slope of the linear portion of the absorption curve, and W_∞ water absorption at saturation time.

The net effect can be calculated in terms of Permeability Coefficient (P) by using Eq. (6):

$$P = D \times S. \quad (6)$$

Experimental modal analysis. Experimental modal analysis has been carried out to study the effect of sisal fiber addition in PLA matrix composites on its natural frequency and damping ratio. In these experiments, a specimen is fixed in rigid support for 20 mm length, a miniature accelerometer is attached to the specimen's free end, and impulse forces are applied using an impact hammer. As a specimen triggered by hammer, the miniature accelerometer measures the displacement signal in the time domain. This time domain signal converts into the frequency domain using Fast Fourier Transform (FFT) algorithm in Bruel & Kjaer DAQ. The direct measurement of FRF was from Photon + software for various weight fraction percentages of fiber-reinforced PP composites. The coherence value was observed to be close to one, confirming the signal's data quality.

As per ASTME 756 [28], the produced composite has undergone impulse excitation analysis. Specimen of 200 × 20 × 3 mm are analysed as cast and shown in Fig. 1(a). The experimental modal analysis determines the natural frequency and associated modal damping as key parameters allied with the dynamic behaviour of the composite structure. The effects of fiber loading on the free vibrational characteristics of composite beams are also investigated.

Figure 1(b) shows a free vibration test setup schematic. The specimen was held with fixed-free boundary conditions, and the excitation was carried out by an impact hammer (PCB Piezoelectric model 086C03) with a hard tip. The lightweight miniature accelerometer (Bruel & Kjaer model 352B10) is used to avoid the effect of the weight of the accelerometer on free vibrational behaviour, and it is placed with wax at the free end of the cantilever beam to acquire displacement signals. The data acquisition system (Bruel & Kjaer with Photon+ software) comprises of fast Fourier transform (FFT) algorithm to get frequency response and time domain signal. The first peaks in Frequency Response Function (FRF) curve show the natural frequency of the studied composite beam. The method employed to find the damping values of sisal fiber-reinforced PLA composites is half-power bandwidth using the FRF curves. Equation (7) was used to calculate a damping ratio.

$$\zeta = \frac{\Delta\omega}{2\omega_n}, \tag{7}$$

where ζ– damping coefficient, $\Delta\omega$ – bandwidth and ω_n– natural frequency.

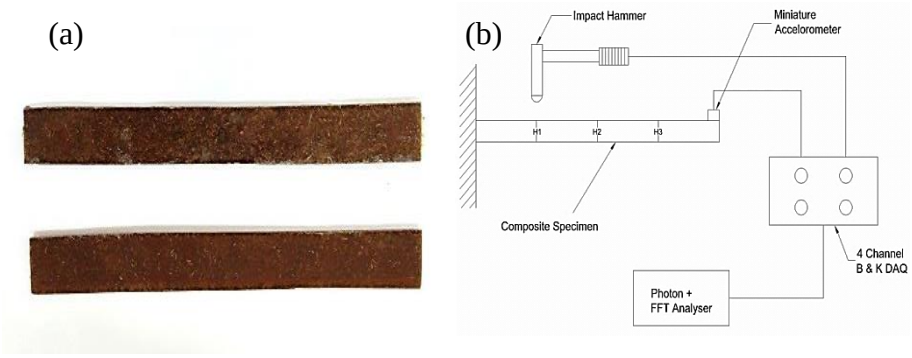

Fig. 1. (a) Test specimen (b) and test setup for experimental modal analysis

Results and Discussion

Density and void fraction. The theoretical and experimental density of the Sisal/PLA composite were obtained and shown in Table 3. For all the compositions, the experimental density was lower than that of theoretical density, and with an increase in fiber content from 10 to 30 %, the density of composites increased. This is because of the higher density of sisal fiber, which is 1.45 g/cm^3, compared to pure PLA, which has 1.24 g/cm^3.

The volume fractions of void content are shown in Table 2. This value indicates the difference in density of composites obtained by the experimental and theoretical methods.

The presence of voids in specimens is mainly because of air trapped during compounding, hollow spaces and incompatibility of fiber with matrix surface.

The value of void content is a maximum of 6.18 %, which clearly shows the fabrication of specimens was fairly good.

Table 3. Density and void content of Sisal/PLA composites

Composition designation	Theoretical Density, g/cc	Experimental Density, g/cc	Volume fraction of voids, %
S10	1.26	1.18	6.18
S20	1.28	1.21	5.04
S30	1.30	1.23	5.23

Shore D hardness. The hardness of composite material is the resistance to indentation. Shore D hardness is the method that relatively measures hardness, a higher number indicates harder material. The value of the hardness of composite material depends on fiber dispersal into the matrix. The hardness of Sisal/PLA is shown in Table 4. Pure PLA exhibited a hardness value of 92.58 lowest, showing it is flexible material phase. Increasing fiber content increases the hardness throughout, and a maximum of was observed for S30 composites 97.28. This shows that the fiber incorporation has reduced the polymer chain's movement of PLA and - increased rigidity.

Table 4. Shore D hardness of PP and sisal/PP composites

Composition designation	Shore D hardness
PLA	92.58
S10	93.84
S20	96.44
S30	97.28

Water absorption. The percentage weight gain versus the square root of time of sisal/PLA composites is shown in Fig. 2. The maximum WA of 4.67 % was seen for S30, and a minimum of 1.30 % for pure PLA. Water absorption (%) increased with an increase in fiber loading. The hydroxyl groups of sisal fiber highly contribute to gaining water. With increased fiber content, the quantity of hydroxyl groups counted to more, promoting an increase in WA. [2,23].

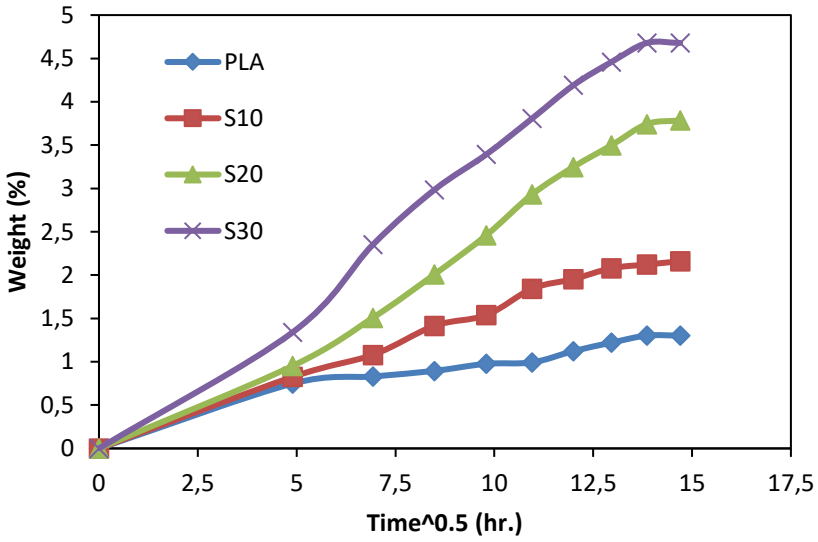

Fig. 2. Water absorption versus time

Table 5. Diffusion and permeability coefficient of the sisal/PLA composites

Composition designation	W_∞	W_t	Diffusion coefficient (D)	Sorption coefficient (S)	Permeability coefficient (P)
PLA	1.302	0.748576	$0.28E^{-05}$	0.575	$1.59E^{-06}$
PLAS10	2.159	0.825318	$1.62E^{-05}$	0.382	$6.21E^{-06}$
PLAS20	3.753	0.921575	$1.78E^{-05}$	0.246	$4.38E^{-06}$
PLAS30	4.678	1.340074	$2.83E^{-05}$	0.286	$8.11E^{-06}$

The diffusion, sorption and permeability coefficient of pure PLA and sisal/PLA composites are depicted in Table 5. The findings discovered that the diffusion coefficient rises with increased fiber content, with the highest for S30 of 2.83E^{-05} mm^2/s. The permeability coefficient has shown similar behavior as that observed for diffusion.

Natural frequency of Sisal/PLA composites. A typical decay curve in the time domain and FRF curve, i.e. FFT of signals respectively for pure PLA shown in Figs. 3 and 4, respectively**.** FRF curve clearly shows the three peaks, the three modes' natural frequency. The beam deformation pattern at each peak is the mode shape which appears to be bending, second bending, and twisting. Similar signal data is obtained by triggering all specimens three times and then average natural frequency values at each mode reported.

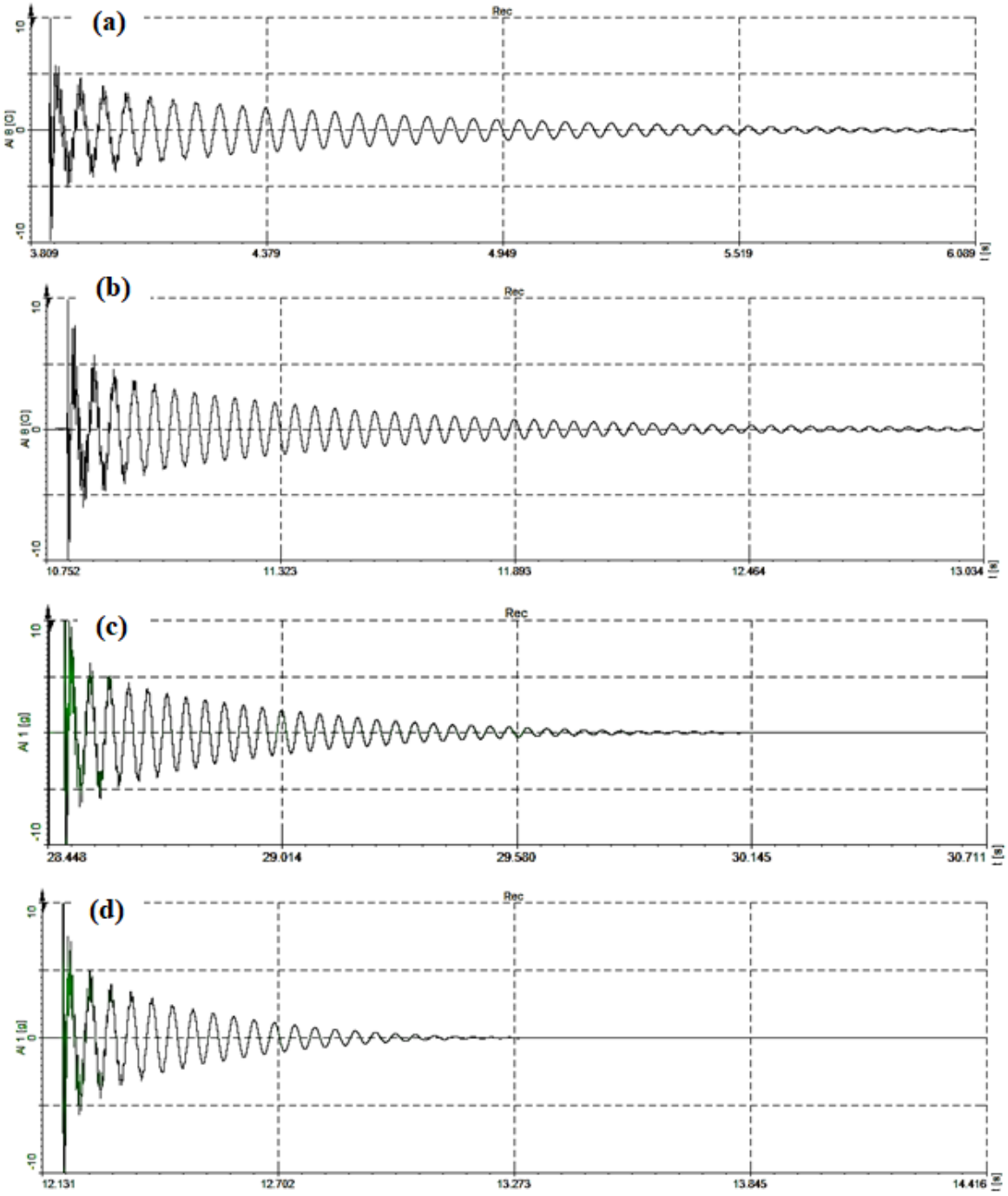

Fig. 3. A time domain signal for pure PLA (a), S10 (b), S20 (c), and S30 (d) composites

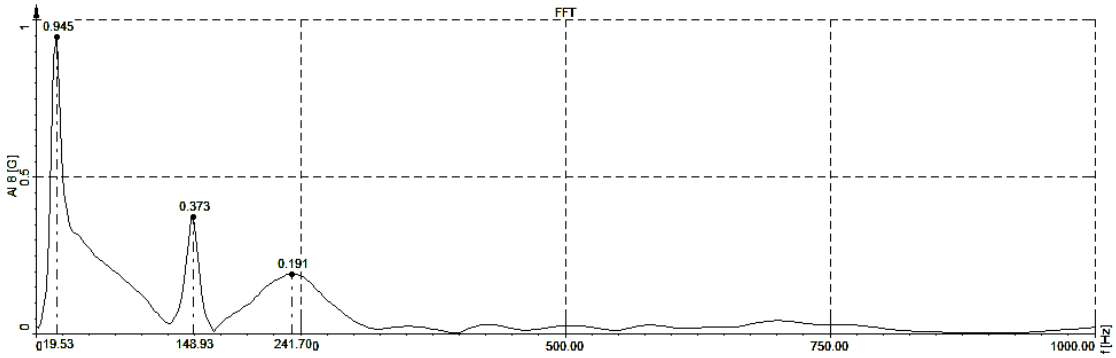

Fig. 4. FRF curve for Pure PLA composites

Figure 5 shows the influence of sisal fiber wt. % on mode one natural frequency of sisal/PLA composites. The mode 1 natural frequency of pure PLA, S10, S20, and S30 are 18.91, 20.75, 23.80, and 24.41 Hz, respectively. The mode 1 natural frequency raised by 9.7, 14.7, and 2.6 % for the subsequent addition of 10 wt. % of sisal over pure PLA.

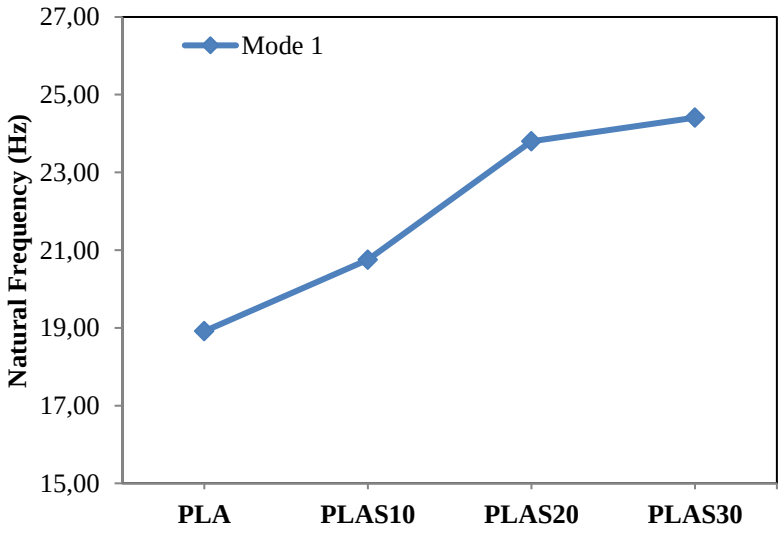

Fig. 5 Influence of fiber wt. % on the natural frequency of composites (Mode1)

Table 6. Influence of wt. % on natural frequency of composites

Composition	Natural frequency, Hz		
	Mode 1	Mode 2	Mode 3
PLA	18.91	148.32	234.38
S10	20.75	168.46	288.70
S20	23.80	180.05	280.15
S30	24.41	172.12	253.90

Table 6 shows that natural frequencies for mode 2 and mode 3 increase with the increase in weight fraction up to 20 wt. % and then slightly decreases but is always higher than the pure PLA composites. This is because of the improved bending stiffness of Sisal/PLA with an increase in fiber content over pure PLA. Also, fiber reinforcement with an increase in fiber loading and the surface-to-surface contact area along the fiber/matrix interface that improves-surfae contact area along the fiber/matrix interface improves stiffness. The decrease in natural frequency of S30 compared to S20 indicated the lowering of stiffness at high fiber content because of the

agglomeration and weakfiber–matrix interface. Similar results for nano clay-filled glass vinyl ester composites were observed by Chandradass et al. (28).

The natural frequency of S10 composites for mode 1, mode 2, and mode 3 is 20.75, 168.46, and 288.70 Hz, respectively. It indicated that the composites exhibited higher natural frequencies when it has higher modes of vibration. A similar trend was observed for pure PLA, S20, and S30 composites.

Damping ratio of sisal/PLA composites. Figure 6 shows the influence of wt. % of fiber on mode 1 damping of PLA composites. The increase in wt. % from 0 to 30 % increases the damping ratio. As fiber content increases, the composite behavior shifts from viscoelastic to elastic and causes a reduction in the damping ratio, but the improvement was observed here. The marginal improvement in damping ratio was observed for S10 and S20 over pure PLA because of higher stiffness. The maximum damping ratio of 0.1450 is obtained at S20, indicating low stiffness, and weakens fibre-matrix interface, making itlose maximum energy. Also, at higher fiber content, there is an increase in the friction at the fibre-matrix interface and interlock of fiber resulting in an increase in damping.

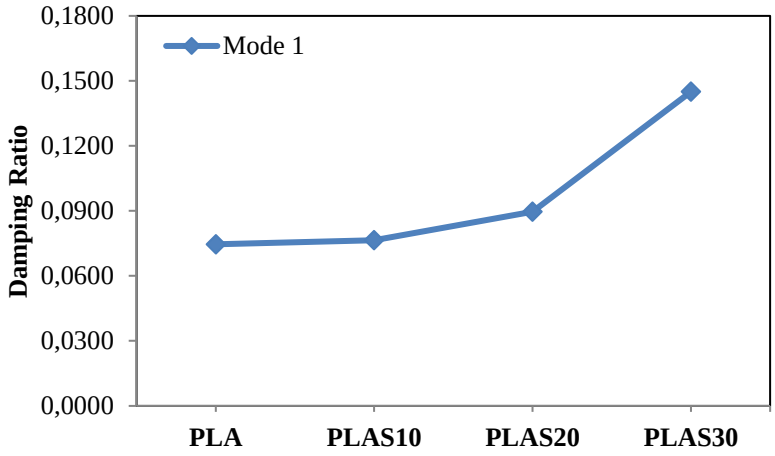

Fig. 6. Influence of wt. % on damping ratio of composites (Mode 1)

Table 7 shows the mode 2 and mode 3 damping ratio of Sisal/PLA composites. It can be seen that a trend of damping for mode 2 and mode 3 is similar to that of mode 1. For pure PLA composites, the damping ratio declined at higher modes of vibration. It is consistent with increased natural frequency at higher mode reducing the damping ratio. A similar trend was observed for S10, S20, and S30 sisal/PLA composites. A similar observation was reported for Banana polyester and sisal polyester composites (29), A Etaati et al. for hemp polypropylene composites (30).

Table 7. Influence of wt. % on damping ratio of composites (Mode 1, 2, 3)

Composition	Damping ratio		
	Mode 1	Mode 2	Mode 3
PLA	0.0746	0.0094	0.0060
S10	0.0764	0.0094	0.0055
S20	0.0896	0.0118	0.0076
S30	0.1450	0.0205	0.0140

Conclusions

In the present research work, Sisal/PLA composite specimens were successfully fabricated by twin screw extrusion and injection molding methods at a different fibre weight fraction. The influence of the weight fraction of sisal fiber in PLA composites on physical and vibration-damping properties was examined. The density and Shore D hardness of PLA composites rise on fiber reinforcement, but at the same time, water absorption also rises to 4.5 % for a 30 % weight fraction of fiber. Fundamental natural frequencies and damping ratio of PLA composites were improved on fiber incorporation. The S30 composition showed the highest natural frequency and damping ratio of 24.41 Hz and 0.1450, respectively. These developed biodegradable composites help lower the cost of purePLA-based composites. The Sisal/PLA composites could be a better alternative for packaging and allied industrial applications.

References

1. Chaitanya S, Singh I. Processing of PLA/sisal fiber biocomposites using direct- and extrusion-injection molding. *Mater. Manuf. Process*. 2017;32(5): 468–474.
2. Bajracharya RM, Bajwa DS, Bajwa SG. Mechanical properties of polylactic acid composites reinforced with cotton gin waste and flax fibers. *Procedia Eng*. 2017;200: 370–376.
3. Rajesh G, Ratna Prasad AV, Gupta A. Mechanical and degradation properties of successive alkali treated completely biodegradable sisal fiber reinforced poly lactic acid composites. *J. Reinf. Plast. Compos*. 2015;34(12): 951–961.
4. Rao KMM, Rao KM, Prasad AVR. Fabrication and testing of natural fibre composites: Vakka, sisal, bamboo and banana. *Mater. Des*. 2010;31(1): 508–513.
5. Rajesh G, Ratna Prasad AV. Tensile Properties of Successive Alkali Treated Short Jute Fiber Reinforced PLA Composites. *Procedia Mater. Science*. 2014;5: 2188–2196.
6. Goriparthi BK, Suman KNS, Mohan Rao N. Effect of fiber surface treatments on mechanical and abrasive wear performance of polylactide/jute composites. *Compos Part A Appl Sci Manuf.* 2012;43(10): 1800–1808.
7. Hu RH, Ma ZG, Zheng S, Li YN, Yang GH, Kim HK, et al. A fabrication process of high volume fraction of jute fiber/polylactide composites for truck liner. *Int. J. Precis Eng, Manuf.* 2012;13(7):1243–1246.
8. Zafar MT, Maiti SN, Ghosh AK. Effect of surface treatment of jute fibers on the interfacial adhesion in poly(lactic acid)/jute fiber biocomposites. *Fibers Polym.* 2016;17(2): 266–274.
9. Shih YF, Huang CC. Polylactic acid (PLA)/banana fiber (BF) biodegradable green composites. *J. Polym. Res*. 2011;18(6): 2335–2340.
10. Hadi A, Radzi M, Akmal N, Saleh M. EP19 Banana Fiber Reinforced Polymer Composites. In: *Empower Sci Technol. Innov. Towar a Better Tomorrow*. 2011. p.192–198.
11. Asaithambi B, Ganesan G, Ananda Kumar S. Bio-composites: Development and mechanical characterization of banana/sisal fibre reinforced poly lactic acid (PLA) hybrid composites. *Fibers Polym*. 2014;15(4): 847–854.
12. Ranjan R, Bajpai PK, Tyagi RK, Tyagi RK. Mechanical Characterization of Banana/Sisal Fibre Reinforced PLA Hybrid Composites for Structural Application. *Eng. Int.* 2013;1(1): 39.
13. Asaithambi B, Ganesan GS, Ananda Kumar S. Banana/sisal fibers reinforced poly(lactic acid) hybrid biocomposites; influence of chemical modification of BSF towards thermal properties. *Polym. Compos*. 2017;38(6): 1053–1062.
14. Du Y, Wu T, Yan N, Kortschot MT, Farnood R. Fabrication and characterization of fully biodegradable natural fiber-reinforced poly(lactic acid) composites. *Compos. Part B Eng.* 2014;56: 717–723.
15. Kaewpirom S, Worrarat C. Preparation and properties of pineapple leaf fiber reinforced poly(lactic acid) green composites. *Fibers Polym*. 2014;15(7): 1469–1477.
16. Chen X, Zhang N, Gu S, Li J, Ren J. Preparation and properties of ramie fabric-reinforced

thermoset poly lactic acid composites. *J. Reinf. Plast. Compos*. 2014;33(10): 953–963.
17. Choi HY, Lee JS. Effects of surface treatment of ramie fibers in a ramie/poly(lactic acid) composite. *Fibers Polym*. 2012;13(2): 217–223.
18. Alam AKMM, Mina MF, Beg MDH, Mamun AA, Bledzki AK, Shubhra QTH. Thermo-mechanical and morphological properties of short natural fiber reinforced poly (lactic acid) biocomposite: Effect of fiber treatment. *Fibers Polym*. 2014;15(6): 1303–1309.
19. Luo H, Xiong G, Ma C, Chang P, Yao F, Zhu Y, Zhang C, Wan Y. Mechanical and thermo-mechanical behaviors of sizing-treated corn fiber/polylactide composites. *Polym. Test.* 2014;39: 45–52.
20. Wang L, Tong Z, Ingram LO, Cheng Q, Matthews S. Green Composites of Poly (Lactic Acid) and Sugarcane Bagasse Residues from Bio-refinery Processes. *J. Polym. Environ*. 2013;21(3): 780–788.
21. Bajpai PK, Singh I, Madaan J. Comparative studies of mechanical and morphological properties of polylactic acid and polypropylene based natural fiber composites. *J. Reinf. Plast. Compos*. 2012;31(24): 1712–1724.
22. Yuan Y, Guo M, Wang Y. Flax Fibers as Reinforcement in Poly (Lactic Acid) Biodegradable Composites. *Commun. Comput. Inf. Sci.* 2011;134(PART 1): 547–553.
23. Bax B, Müssig J. Impact and tensile properties of PLA/Cordenka and PLA/flax composites. *Compos. Sci. Technol*. 2008;68(7–8): 1601–1607.
24. Huda MS, Drzal LT, Mohanty AK, Misra M. Effect of fiber surface-treatments on the properties of laminated biocomposites from poly(lactic acid) (PLA) and kenaf fibers. *Compos Sci Technol*. 2008;68(2): 424–432.
25. Lee SH, Wang S. Biodegradable polymers/bamboo fiber biocomposite with bio-based coupling agent. *Compos Part A Appl Sci Manuf.* 2006;37(1): 80–91.
26. Ambone T, Joseph S, Deenadayalan E, Mishra S, Jaisankar S, Saravanan P. Polylactic Acid (PLA) Biocomposites Filled with Waste Leather Buff (WLB). *J. Polym. Environ.* 2017;25(4): 1099–1109.
27. Koutsomitopoulou AF, Bénézet JC, Bergeret A, Papanicolaou GC. Preparation and characterization of olive pit powder as a filler to PLA-matrix bio-composites. *Powder Technol*. 2014;255: 10–16.
28. Chandradass J, Ramesh Kumar M, Velmurugan R. Effect of clay dispersion on mechanical, thermal and vibration properties of glass fiber-reinforced vinyl ester composites. *J. Reinf. Plast. Compos*. 2008;27(15): 1585–1601.
29. Senthil Kumar K, Siva I, Jeyaraj P, Winowlin Jappes JT, Amico SC, Rajini N. Synergy of fiber length and content on free vibration and damping behavior of natural fiber reinforced polyester composite beams. *Mater Des*. 2014;56: 379–386.
30. Etaati A, Pather S, Fang Z, Wang H. The study of fibre/matrix bond strength in short hemp polypropylene composites from dynamic mechanical analysis. *Compos. Part B Eng*. 2014;62: 19–28.

THE AUTHORS

Munde Yashwant
e-mail: yashwant.munde@gmail.com

A.S. Shinde
e-mail: avinash.shinde@cumminscollege.in

I. Siva
e-mail: isiva@klu.ac.in

Prashant Anerao
e-mail: prashant.anerao@viit.ac.in